Journal of Materials Chemistry

Cite this: J. Mater. Chem., 2011, 21, 17236

www.rsc.org/materials

PAPER

Electric transport, reversible wettability and chemical sensing of single-crystalline zigzag Zn_2SnO_4 nanowires

Di Chen,[a] Jing Xu,[a] Bo Liang,[a] Xianfu Wang,[a] Po-Chiang Chen,[b] Chongwu Zhou*[b] and Guozhen Shen*[a]

Received 27th July 2011, Accepted 20th August 2011
DOI: 10.1039/c1jm13579a

Ternary oxides have the advantages of tuning their physical properties by varying the proportion of each component, thus attracting great research attention in recent years. As an example, we demonstrated in this work the investigation on the electronic transport, surface wettability and chemical sensing properties of zigzag Zn_2SnO_4 nanowires, which were synthesized from a thermal evaporation method. Structural characterizations reveal that these nanowires are single crystals with average diameters of ~100 nm and grow along the [1$\bar{1}$1] direction. Single nanowire-based field effect transistor was fabricated, showing an on/off ratio of 10^4 and a device mobility of 17.2 cm^2 $(V\ s)^{-1}$. Besides, these Zn_2SnO_4 nanowire-based devices showed a substantial increase in conductance upon exposure to UV light. Thin films of the zigzag Zn_2SnO_4 nanowires were configured as high performance sensors to detect hosts of chemicals with detection limits down to the 1 ppm level, especially for ethanol and acetone, implying promising applications in detecting toxic volatile organic compounds.

Introduction

Due to their special shapes, compositions, chemical and physical properties as well as their promising applications in the fabrication of nanoscale devices, one-dimensional (1-D) metal oxide nanostructures have attracted immense interest since they are the commonest minerals in the earth.[1–10] 1-D metal oxide nanostructures have now been widely used in many areas, such as ceramics, catalysis, sensors, photodetectors, transparent conductive films, photocatalysts, electro-optical and electrochromic devices.[11–20] To date, intensive studies have been carried out on the synthesis of 1-D binary oxide nanostructures as well as the exploration of their novel properties, for example, ZnO, In_2O_3, SnO_2, Ga_2O_3, TiO_2, Cu_2O and WO_3.[11–20] However, in comparison with simple binary oxides, there are still very few studies concerning ternary oxides nanostructures,[21–25] though ternary oxides have more freedom to tune the materials' chemical and physical properties by altering the compositions.

The ternary Zn–Sn–O crystal exists in two phases, spinel-type structured Zn_2SnO_4 and ilmenite-type structured $ZnSnO_3$, under normal pressure at room temperature.[26,27] Studies verified that bulk Zn_2SnO_4 crystal has a high thermal stability, high electron mobility, and low visible absorption. Zn_2SnO_4 has potential applications as electronic and optoelectronic devices including solar cells, chemical sensors, photodetectors, photocatalysts, and Li-ion batteries. With 1-D nanoscale shapes, they may have enormous potential to work as building blocks for nanoelectronics, and are expected to offer superior chemical sensing and photoconducting performance due to the enhanced surface to volume ratio.[28–40] Despite the utmost importance, only relatively small efforts have been directed toward the synthesis of 1-D Zn_2SnO_4 nanostructures, such as nanowires, and nanobelts,[28–40] and there is still a lack of efficient investigation on the device applications of 1-D Zn_2SnO_4 nanostructures.

In this work, n-type field-effect transistors (FET), with an on/off ratio of 10^4 and a device mobility of 17.2 cm^2 $(V\ s)^{-1}$, were fabricated on a single zigzag Zn_2SnO_4 nanowire prepared *via* a thermal evaporation method. Besides, these devices showed a substantial increase in conductance upon exposure to UV light. Fast photoinduced switching surface wettability was observed for the nanowire films and the contact angle decreased from 122° to 0° within 40 min. Thin films of the zigzag Zn_2SnO_4 nanowires were configured as high performance resister-type sensors, which can be used to detect hosts of chemicals. Especially, the detection limit was found to be as low as 1 ppm level for ethanol and acetone, implying promising applications in detecting toxic volatile organic compounds.

Experimental section

Zigzag single-crystalline Zn_2SnO_4 nanowires were synthesized *via* a simple catalyst-free vapor-solid method. In a typical process, a mixture of 0.065 g Zn and 0.335 g SnO, serving as the source material, were placed in a quartz boat located inside a 1-inch-diameter quartz tube reactor. Si/SiO_2 substrate was then placed face-down above the source material to ensure high vapor pressure and to collect the product. The furnace was then raised

[a]*Wuhan National Laboratory for Optoelectronics and College of Optoelectronic Science and Engineering, Huazhong University of Science and Technology, Wuhan, 430074, China. E-mail: gzshen@mail.hust.edu.cn*
[b]*Department of Electrical Engineering, University of Southern California, Los Angeles, California, 90089, United States. E-mail: chongwuz@usc.edu*

to 920 °C and kept at that temperature for 2 h. After reaction, white product was found deposited on the substrate and collected for characterization by using scanning electron microscopy (SEM, Hitachi S4800) and transmission electron microscopy (TEM, JEOL JEM-3000F) equipped with an energy-dispersive X-ray spectrometer (EDS). The surface wettability was investigated by measuring the water contact angle by an SL200B contact angle system (Solon Technology Science Co., Ltd.) at ambient pressure and room temperature.

To prepare the individual zigzag nanowire FET for electrical performance testing, the as-prepared nanowires grown on silicon substrate were sonicated in a suspension in isopropanol (IPA) and then dropped onto a degenerately doped silicon wafer covered with 500 nm SiO_2. Subsequently, photolithography was performed to pattern the source–drain electrodes, followed by thermal deposition of Ti/Au contact pads with thickness of 5 nm/100 nm. The transport properties were measured by a probe station with an Agilent 4156B semiconductor characterization system.

For fabricating the gas sensors, some Zn_2SnO_4 nanowires were mixed with a suitable amount of ethanol to form a white paste after being sonicated. The pastes were coated onto alumina ceramic tubes with a pair of Pt electrodes attached for resistance measurements. After being welded on the pedestal, the gas sensors were aged for 72 h by applying 5 V on the heating wire. The sensors were then measured with a self-made chemical sensing system. During the test, a load resistor and a constant working voltage at 5 V was applied to the system. By measuring the across voltage of the load resistor, the electrical resistance of the Zn_2SnO_4 nanowires sensors can be calculated by Ohm's law: $R_S = (5/V_O - 1)R_L$. The sensitivity (S) was defined as $S = R_a/R_g$, where R_a is the sensor resistance in air and R_g is the resistance in target gas atmosphere. After putting the sensors in a gas chamber, the measurement was processed by injecting target gases with different concentrations at the optimum temperature.

Results and discussion

After synthesis, white products were found deposited on the silicon substrate. X-ray diffraction studies reveal that they are pure face-centered cubic structured Zn_2SnO_4 phase. Fig. 1a shows a SEM image of the as-synthesized Zn_2SnO_4 product, which reveals the formation of 1-D wire-like materials with diameters of 100–200 nm and lengths of several hundred micrometres. Fig. 1b is a high-magnification SEM image, showing several typical synthesized wires. From these images, it can be seen that most of the 1-D Zn_2SnO_4 nanostructures are nanowires with interesting zigzag shapes, instead of the commonly straight nanowires. Higher magnification SEM images of two typical zigzag nanowires are depicted in Fig. 1c and 1d, respectively, where the periodical morphologies can be clearly seen. In fact, from the images, we can see that the whole nanowires are actually formed by a row of inlaid uniform rhombohedral nanocrystals along their axial direction, organized into ordered steps on the surface of the nanowires with average diameters of ~100 nm. A typical EDX spectrum of the Zn_2SnO_4 nanowires is shown in Fig. 1e, confirming the formation of pure Zn_2SnO_4 products.

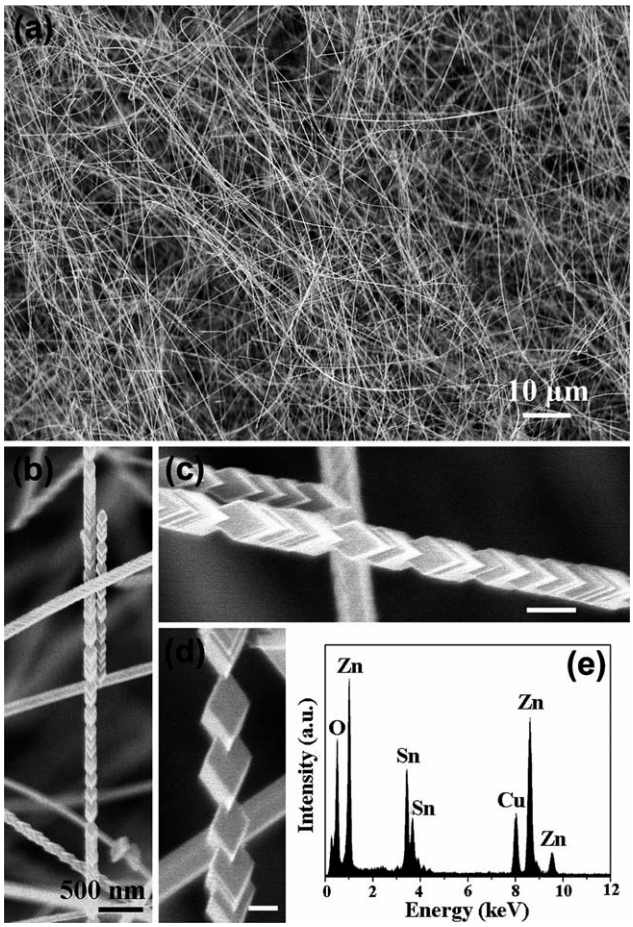

Fig. 1 SEM images with different magnifications of the synthesized zigzag Zn_2SnO_4 nanowires on a large scale. Scale bars for (c,d): 100 nm.

The microstructures of the synthesized Zn_2SnO_4 nanowires were studied by TEM and the corresponding images are depicted in Fig. 2. Fig. 2a and 2b show the TEM images of two zigzag Zn_2SnO_4 nanowires, both of which are formed by several rhombohedral nanocrystals along the axis of the nanowires, in accordance with the SEM result. Selected-area electron diffractions (SAED) taken from the two nanowires are shown in Fig. 2a inset, revealing their single crystalline nature. Lattice-resolved high-resolution TEM (HRTEM) images of the parts framed in Fig. 2b are demonstrated in Fig. 2c and 2d, respectively. Three groups of clearly resolved lattice fringes are calculated to be around 0.50 nm, 0.50 nm and 0.43 nm, corresponding to the $(\bar{1}11)$, $(1\bar{1}1)$ and (002) planes of face-centered cubic Zn_2SnO_4 phase. The results indicate the formation of single crystalline Zn_2SnO_4 nanowires with the preferred growth directions along the $[1\bar{1}1]$ planes.

Since no catalyst was used in the reaction, a vapor-solid (VS) process should be the dominant mechanism. The growth process of the zigzag Zn_2SnO_4 nanowires can be expressed as follows. At high reaction temperature, Zn and SnO reacted with the residual oxygen in the system to form Zn_2SnO_4 octahedral nanocrystals, which tend to grow along the $[\bar{1}11]$, $[11\bar{1}]$, and [002] directions, as indicated in Fig. 2e. The newly formed Zn_2SnO_4 octahedral nanocrystals then grow rapidly along the $[1\bar{1}1]$ direction and finally stretch into a zigzag shaped nanowire. Similar results were

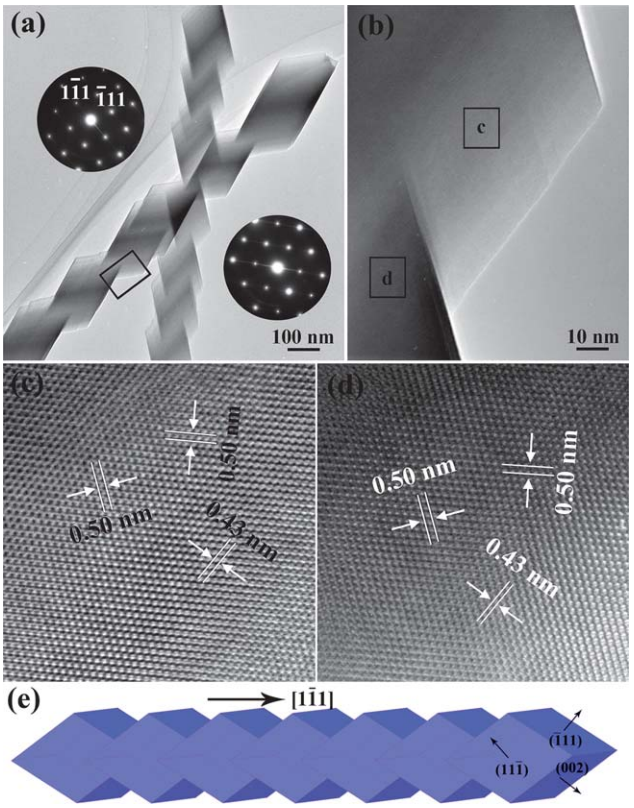

Fig. 2 (a) TEM image of the zigzag Zn_2SnO_4 nanowires. Inset is the corresponding SAED patterns. (b) High-magnification TEM image taken from the frame marked in (a). (c,d) HRTEM images taken from the parts framed in (b). (e) Schematic illustration of the growth of zigzag Zn_2SnO_4 nanowires.

observed for the formation of zigzag Zn_2SnO_4 nanowires from the vapor-liquid-solid (VLS) process in the presence of gold nanoparticles.[30]

As an important wide band gap transparent semiconductor, Zn_2SnO_4 has great applications in electronic and optoelectronic devices.[39,40] Here, we first fabricated single Zn_2SnO_4 nanowire based FETs directly on Si/SiO_2 substrate to investigate its electric transport properties. The upper-left inset in Fig. 3a is a SEM image of the single nanowire FET device. The channel width of the device is 1.5 μm. Fig. 3a shows the drain current (I_{ds}) *versus* source–drain voltage (V_{ds}) curves of a typical device. Linear current *vs.* voltage is obtained, indicating very good Ohmic contacts between the electrodes and the nanowire. The applied gate voltages range from −30 V to 30 V with an average step of 5 V. From the curves, the conductance of the device increased gradually with increased gate voltages, indicating n-type semiconducting behaviors. The I_{ds}–V_g curve was also measured and the curve was shown in Fig. 3a inset (bottom right). The on/off ratio is around 10^4. Calculated from the curve, the device mobility was found to be around 17.2 cm^2 $(V\ s)^{-1}$, which is a bit higher than the previously reported one on straight Zn_2SnO_4 nanowire from the VLS process.[39]

Photoconducting properties of the as-synthesized zigzag Zn_2SnO_4 nanowires were also studied by exposing the nanowire FETs with a UV lamp of 254 nm in wavelength. A schematic diagram of the photodetecting device is shown in Fig. 3b inset.

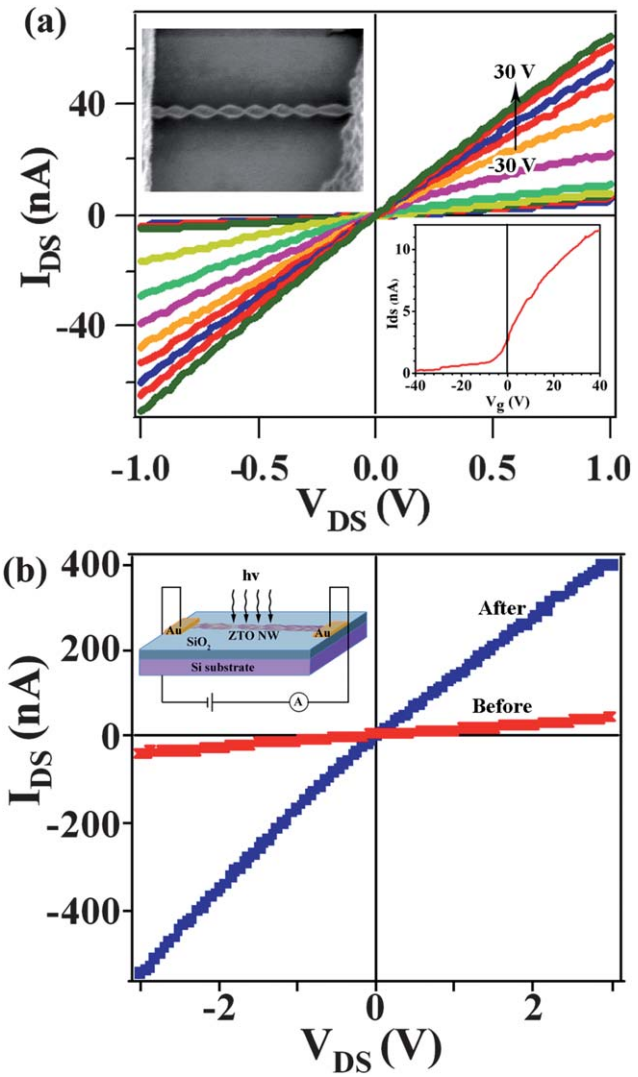

Fig. 3 (a) I_{DS}–V_{DS} curves measured at different gate voltages with a step of 5 V. Insets are the corresponding SEM image of the device and I_{DS}–V_G transfer curve, respectively. (b) *I–V* curves of the Zn_2SnO_4 nanowire device measured before and after UV light illumination, respectively.

Fig. 3b shows the *I–V* curves measured with (blue curve) and without (red curve) UV light irradiation, where the device conductance was found to increase immediately upon exposure to UV light irradiation. At a voltage of 4 V, the measured current of the device is up to 593 nA under UV light irradiation, while the value is around 34 nA in the dark. The current increased over ten times with the UV light irradiation, indicating their possible applications in photoswitches, optical imaging technique, and optoelectronic circuits. The increase in current under light irradiation can be expressed as follows. For a zigzag Zn_2SnO_4 nanowire exposed to air, O_2 adsorbs on the nanowire surface and combines with the nearby free electrons to form an O_2^- layer on its surface. Thus it subsequently reduced the conductivity of the zigzag Zn_2SnO_4 nanowire. Upon exposure to UV light, the O_2^- ions first recombine with the photogenerated holes, discharge O_2 molecules from the surface, and the process brings the nanowire to the original electron-rich state. Further illumination with UV light generates more electron–hole pairs in the conduction and

valence bands, thus significantly increase the conductance of the nanowire.[41–45]

Surface wettability of nanostructures, in terms of contact angle (CA), is one of the most important properties of nanostructured films.[46–48] The surface wettability of the as-synthesized zigzag Zn_2SnO_4 nanowires was also investigated by measuring the contact angle of a water droplet on the nanowire film. Fig. 4a is the corresponding result. The CA was measured to be 122°, indicating its hydrophobic behavior. According to previous reports, the CA was mainly governed by two factors. One is the chemical composition and the other is the roughness of the surface. The surface roughness of the current zigzag Zn_2SnO_4 nanowires film is also thought to be the key reason for its hydrophobic behavior since the surface roughness contained enough room to hold air in the troughs between nanowires. Similar results were also obtained for many binary oxide nanowires, including In_2O_3, SnO_2, ZnO, and so on.[49–55]

The photoinduced wettability conversion of the as-synthesized zigzag Zn_2SnO_4 nanowires was also studied. Fig. 4b presents the conversion of the CA during UV illumination. It was found that, when the nanowire film is exposed to UV light, the CA gradually decreased from 122° to 0° with the increase of exposure time. The hydrophobic-superhydrophilic transition occurred within 40 min and it can be recovered in 20 min in the dark. Several cycles were performed, confirming the reversible wettability switching behavior between hydrophobic and superhydrophilic surface properties. The fast surface wettability transition of the current zigzag Zn_2SnO_4 nanowires might be improved to be applied in the sensitive smart switches. It is well-known that UV illumination will generate electron–hole pairs in the Zn_2SnO_4 nanowire surface—some of the holes can react with lattice oxygen to form surface oxygen vacancies. The defective sites are kinetically more favorable for polar water molecules than oxygen molecules, which lead to dissociative adsorption of the water molecules on the surface. However, in the dark periods, the hydroxyl groups adsorbed on the defective sites can be replaced gradually by oxygen atoms due to their instability. As a consequence, the wettability of the Zn_2SnO_4 nanowire surface can be switched.

Trace detection of chemicals, like industrial gases, and chemical warfare agents, is an important issue to human health and safety.[56–61] Sensing behavior is one of the most important and well-known properties of metal oxide materials and it was found that metal oxide sensors usually demonstrate much higher sensitivity to their chemical environment than the other chemical sensors in their sensitivity, selectivity, and stability. The gas sensing properties of the zigzag Zn_2SnO_4 nanowires were also studied by configuring the nanowires into thin film type sensors. Fig. 5a shows the representative dynamic gas response of the Zn_2SnO_4 gas sensor to ethanol with concentrations ranging from 1 ppm to 200 ppm. Seven cycles were successively recorded, corresponding to ethanol gases with the concentrations of 1, 5, 10, 50, 100, 150, and 200 ppm, respectively. From the curves, it can be seen that the conductance of the sensor undergoes a drastic rise upon the injection of ethanol and rapidly drops to its initial state after the sensor was exposed to air. The sensitivity of the sensor to 1 ppm ethanol is around 2 and to 200 ppm ethanol is around 27, respectively. The gas sensing response and recovery times of the Zn_2SnO_4 gas sensor were also studied, which are believed to be the two important parameters to evaluate the performance of a gas sensor. From Fig. 5b, we can see that the sensing response and recovery times were 7 s and 8 s for 50 ppm ethanol, respectively, indicating the fast sensing ability of the current nanowire sensors. The values are comparable to previously reported flower-like Zn_2SnO_4 nanostructures (10–15 nm in diameter) and $ZnSnO_3$ nanowires (20–90 nm in diameter) though our zigzag nanowires in this work have relatively larger diameters.[35,62] We believe that the special zigzag shapes of our nanowires contributed to the good sensing performance.

The sensing ability of the Zn_2SnO_4 nanowire sensor to acetone with different concentrations was also studied. The detection limit to acetone was found to be 1 ppm. Fig. 5c is the dynamic gas response of the Zn_2SnO_4 nanowire sensor to acetone with concentrations ranging from 1 ppm to 200 ppm, respectively. Similar to the detection of ethanol, the conductance of the sensor also undergoes a drastic rise upon the injection of gases and drops to its initial state after the sensor was exposed to air.

Similar to the sensing mechanism of binary oxide chemical sensors, we explained the sensing mechanism of the Zn_2SnO_4 nanowire sensor as follows. Once the sensor was exposed to air at high temperature, oxygen molecules were adsorbed on the Zn_2SnO_4 surface, which were reduced to generate ionized oxygen species, such as O_2^-, or O^-, through trapping electrons from the conductance band of Zn_2SnO_4. As a result, the conductivity of the Zn_2SnO_4 nanowires decreased. Once reduction gases, such as ethanol, were introduced into the sensing system, the approached gas molecules reacted with the generated ionized oxygen species, which resulted in the release of electrons to the surface layer of Zn_2SnO_4. Thus, the conductivity of the Zn_2SnO_4 nanowires was increased gradually.

We also measured the response of the zigzag Zn_2SnO_4 nanowire based gas sensor to other volatile organic compounds with a fixed concentration of 100 ppm, such as methanol, methylbenzene, chloroform, styrene, formic acid, acetic acid, and formaldehyde. As shown in Fig. 5d, different sensitivities were obtained for different chemicals and the sensing response and recovery time are also quite short. We believed that the as-prepared zigzag Zn_2SnO_4 nanowires may have potential applications in the detection of volatile organic compounds.

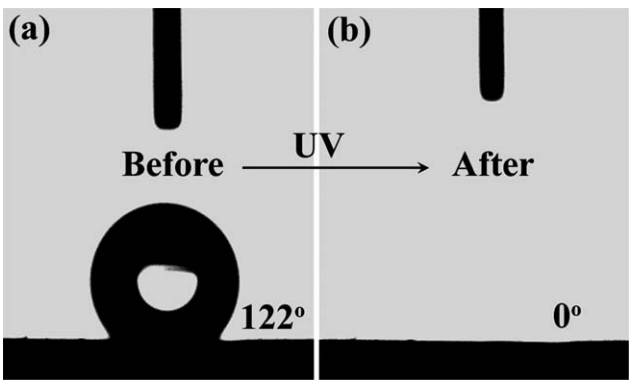

Fig. 4 Photoinduced reversible wettability of the zigzag Zn_2SnO_4 nanowires. (a) Before and (b) after UV illumination.

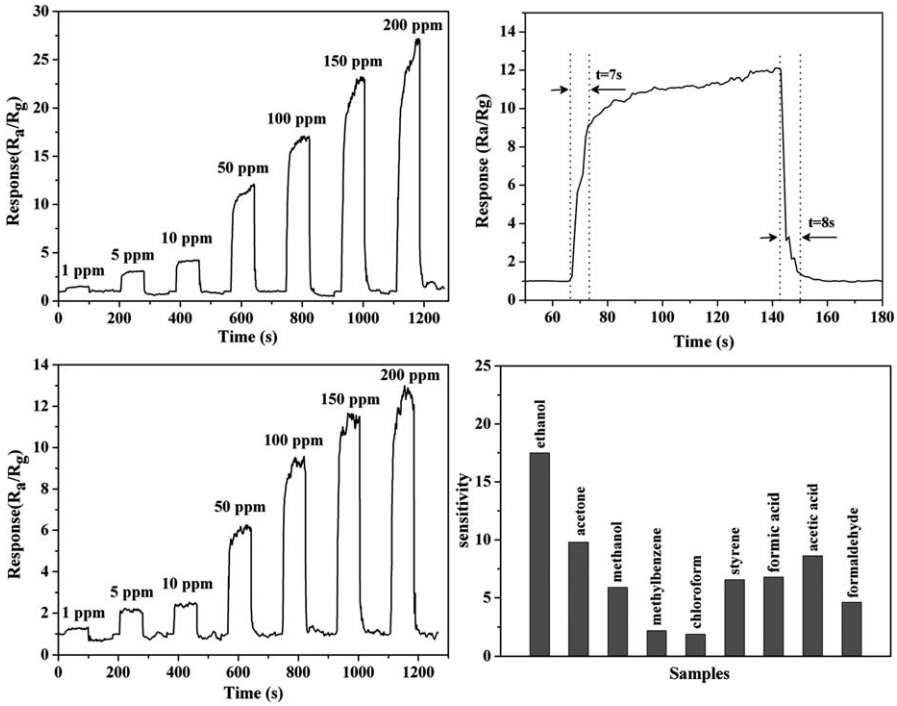

Fig. 5 (a) Dynamic response–recovery curves of the gas sensors to ethanol with varied concentrations. (b) Dynamic response–recovery curves of the gas sensors to 50 ppm ethanol. (c) Dynamic response–recovery curves of the gas sensors to acetone with varied concentrations. (d) Sensing response of the gas sensors to different gases with a concentration of 100 ppm.

Conclusions

In conclusion, single nanowire based FETs were fabricated by using single crystalline zigzag Zn_2SnO_4 nanowires, obtained from catalyst-free vapor-solid method, as the active material. An on/off ratio of 10^4 and a high device mobility of 17.2 cm^2 $(V\ s)^{-1}$ were obtained from the device. Upon UV light irradiation, the current of the device increased over ten times from 34 nA in the dark to 593 nA in light irradiation. Surface wettability studies showed the hydrophobic behavior with an average CA of about 122°, with the feature of fast photoinduced reversible switching between hydrophobic to hydrophilic. Besides, the obtained zigzag Zn_2SnO_4 nanowires exhibited excellent gas sensing performance towards ethanol and acetone with detection limits around 1 ppm. Our results suggest that the zigzag Zn_2SnO_4 nanowires may find great applications in electronic and opto-electronic devices, such as high performance photodetectors, photo switches, as well as chemical sensors to detect toxic volatile organic compounds.

Acknowledgements

This work was supported by the National Natural Science Foundation of China (51002059, 21001046, 91123008), the 973 Projects of China (2011CBA00703, 2011CB933300), the Research Fund for the Doctoral Program of Higher Education (20090142120059, 20100142120053), the Natural Science Foundation of Hubei Province (2009CDB326), the Basic Scientific Research Funds for Central Collges (2010QN045), and the Director Fund of WNLO. Special thanks to the Analytical and Testing Center of HUST.

Notes and references

1 Z. Pan, Z. Dai and Z. L. Wang, *Science*, 2001, **291**, 1947.
2 G. R. Patzke, F. Krumeich and R. Nesper, *Angew. Chem., Int. Ed.*, 2002, **41**, 2446.
3 G. Z. Shen, J. Xu, X. F. Wang, H. T. Huang and D. Chen, *Adv. Mater.*, 2011, **23**, 771.
4 L. Vayssieres, *Adv. Mater.*, 2003, **15**, 464.
5 D. F. Zhang, L. D. Sun, J. L. Yin and C. H. Yan, *Adv. Mater.*, 2003, **15**, 1022.
6 Z. Liu, D. Zhang, S. Han, C. Li, T. Tang, W. Jin, X. Liu, B. Lei and C. Zhou, *Adv. Mater.*, 2003, **15**, 1754.
7 Y. Yin, G. Zhang and Y. N. Xia, *Adv. Funct. Mater.*, 2002, **12**, 293.
8 H. Imai, Y. Takei, K. Shimizu, M. Matsuda and H. Hirashima, *J. Mater. Chem.*, 1999, **9**, 2971.
9 P. Yang and C. M. Lieber, *Science*, 1996, **273**, 1836.
10 M. H. Huang, S. Mao, H. l Feick, H. Yan, Y. Wu, H. Kind, E. Weber, R. Russo and P. Yang, *Science*, 2001, **292**, 1897.
11 P. Chang, Z. Fan, C. Chien, D. Stichtenoth, C. Ronning and J. G. Lu, *Appl. Phys. Lett.*, 2006, **89**, 133113.
12 D. Chen, J. Xu, Z. Xie and G. Z. Shen, *ACS Appl. Mater. Interfaces*, 2011, **3**, 2112.
13 J. Liu, Y. Li, F. J. Fan, Z. Zhu, J. Jiang, R. Ding, Y. Hu and X. T. Huang, *Chem. Mater.*, 2010, **22**, 212.
14 H. J. Fan, W. Lee, R. Hauschild, M. Alexe, R. Scholz, A. Dadgar, K. Nielsch, H. Kalt, A. Krost, M. Zacharias and U. Gosele, *Small*, 2006, **2**, 561.
15 Z. Fan and J. G. Lu, *IEEE Trans. Nanotechnol.*, 2006, **5**, 393.
16 L. Liao, Z. Zhang, B. Yan, Z. Zheng, Q. L. Bao, T. Wu, C. M. Li, Z. X. Shen, J. X. Zhang, H. Gong, J. C. Li and T. Yu, *Nanotechnology*, 2009, **20**, 085203.
17 L. Liao, Z. Zheng, B. Yan, J. X. Zhang, H. Gong, J. C. Li, C. Liu, Z. X. Shen and T. Yu, *J. Phys. Chem. C*, 2008, **112**, 10784.
18 Z. L. Wang, *Mater. Today*, 2004, **7**, 26.
19 X. D. Wang, J. Song, J. Liu and Z. L. Wang, *Science*, 2007, **316**, 102.
20 C. Xu, J. Wu, U. V. Desai and D. Gao, *J. Am. Chem. Soc.*, 2011, **133**, 8122.

21 L. Li, E. Auer, M. Liao, X. Fang, T. Zhai, U. K. Gautam, A. Lugstein, Y. Koide, Y. Bando and D. Golberg, *Nanoscale*, 2011, **3**, 1120.
22 G. Shen and D. Chen, *J. Am. Chem. Soc.*, 2006, **128**, 11762.
23 P. Feng, J. Zhang, Q. Wan and T. H. Wang, *J. Appl. Phys.*, 2007, **102**, 074309.
24 D. Chen and J. H. Ye, *Chem. Mater.*, 2009, **21**, 2327.
25 S. Y. Bae, J. Lee, H. Jung, J. Park and J. P. Ahn, *J. Am. Chem. Soc.*, 2005, **127**, 10802.
26 T. J. Coutts, D. L. Young, X. Li, W. P. Mulligan and X. Wu, *J. Vac. Sci. Technol., A*, 2000, **18**, 2646.
27 J. H. Yu and G. M. Choi, *Sens. Actuators, B*, 2001, **72**, 141.
28 Y. Li and X. L. Ma, *Phys. Status Solidi A*, 2005, **202**, 435.
29 L. Wang, X. Zhang, X. Liao and W. Yang, *Nanotechnology*, 2005, **16**, 2928.
30 J. Wang, X. W. Sun, S. Xie, W. Zhou and Y. Yang, *Cryst. Growth Des.*, 2008, **8**, 707.
31 K. R. G. Karthik, B. P. Andreasson, C. Sun, S. S. Pramana, B. Varghese, C. H. Sow, N. Mathews, L. H. Wong and S. G. Mhaisalkar, *Electrochem. Solid-State Lett.*, 2011, **14**, K5.
32 H. Chen, J. Wang, H. Yu, H. Yang, S. Xie and J. Li, *J. Phys. Chem. B*, 2005, **109**, 2573.
33 J. Jie, G. Wang, X. Han, J. Fang, Q. Yu, Y. Liao, B. Xu, Q. Wang and J. G. Hou, *J. Phys. Chem. B*, 2004, **108**, 8249.
34 H. Zhu, D. Yang, G. Yu, H. Zhang, D. Jin and K. Yao, *J. Phys. Chem. B*, 2006, **110**, 7631.
35 Z. Chen, M. Cao and C. Hu, *J. Phys. Chem. C*, 2011, **115**, 5522.
36 J. W. Zhao, L. R. Qin and L. D. Zhang, *Solid State Commun.*, 2007, **141**, 663.
37 J. X. Wang, S. S. Xie, H. J. Yuan, X. Q. Yan, D. F. Liu, Y. Gao, Z. P. Zhou, L. Song, L. F. Liu, X. W. Zhao, X. Y. Dou, W. Y. Zhou and G. Wang, *Solid State Commun.*, 2004, **131**, 435.
38 Y. Su, L. Zhu, L. Xu, Y. Chen, H. Xiao, Q. Zhou and Y. Feng, *Mater. Lett.*, 2007, **61**, 351.
39 C. Pang, B. Yan, L. Liao, B. Liu, Z. Zheng, T. Wu, H. Sun and T. Yu, *Nanotechnology*, 2010, **21**, 465706.
40 Y. Zhang, J. Wang, H. Zhu, H. Li, L. Jiang, C. Shu, W. Hu and C. Wang, *J. Mater. Chem.*, 2010, **20**, 9858.
41 L. Li, Y. Zhang, X. Fang, T. Zhai, M. Liao, X. Sun, Y. Koide, Y. Bando and D. Golberg, *J. Mater. Chem.*, 2011, **21**, 6525.
42 G. Z. Shen and D. Chen, *J. Mater. Chem.*, 2010, **20**, 10888.
43 P. Irvin, Y. Ma, D. F. Bogorin, C. Cen, C. W. Bark, C. M. Folkman, C. B. Eom and J. Levy, *Nat. Photonics*, 2010, **4**, 849.
44 T. Zhai, L. Li, X. Wang, X. Fang, Y. Bando and D. Golberg, *Adv. Funct. Mater.*, 2010, **20**, 4233.
45 G. Shen and D. Chen, *Recent Pat. Nanotechnol.*, 2010, **4**, 20.
46 W. Zhu, X. Feng, L. Feng and L. Jiang, *Chem. Commun.*, 2006, 2753.
47 J. Niu and J. Wang, *Cryst. Growth Des.*, 2008, **8**, 2793.
48 M. Miyauchi, A. Nakajima, T. Watanabe and K. Hashimoto, *Chem. Mater.*, 2002, **14**, 2812.
49 M. Zhong, M. Zheng, A. Zeng and L. Ma, *Appl. Phys. Lett.*, 2008, **92**, 093118.
50 B. Yan, J. Tao, C. Pang, Z. Zheng, Z. Shen, C. H. Alfred Huan and T. Yu, *Langmuir*, 2008, **24**, 10569.
51 J. Xu, Y. Zhu, H. Huang, Z. Xie, D. Chen and G. Shen, *CrystEngComm*, 2011, **13**, 2629.
52 F. M. Chang, S. L. Cheng, S. J. Hong, Y. J. Sheng and H. K. Tsao, *Appl. Phys. Lett.*, 2010, **96**, 114101.
53 G. Shen, B. Liang, X. Wang, H. Huang, D. Chen and Z. L. Wang, *ACS Nano*, 2011, **5**, 6148.
54 A. C. Chen, X. S. Peng, K. Koczkur and B. Miller, *Chem. Commun.*, 2004, 1964.
55 G. Kenanakis, E. Stratakis, K. Vlachou, D. Vernardou, E. Koudoumas and N. Katsarakis, *Appl. Surf. Sci.*, 2008, **254**, 5695.
56 G. Shen, B. Liang, X. Wang, P. C. Chen and C. Zhou, *ACS Nano*, 2011, **5**, 2155.
57 A. Kolmakov, Y. Zhang, G. Cheng and M. Moskovits, *Adv. Mater.*, 2003, **15**, 997–1000.
58 V. V. Sysoev, J. Goschnick, T. Schneider, E. Strelcov and A. Kolmakov, *Nano Lett.*, 2007, **7**, 3182–3188.
59 C. Li, D. Zhang, X. Liu, S. Han, T. Tang, J. Han and C. Zhou, *Appl. Phys. Lett.*, 2003, **82**, 1613.
60 Z. Fan and J. G. Lu, *Appl. Phys. Lett.*, 2005, **86**, 123510.
61 D. Zhang, Z. Liu, C. Li, T. Tang, X. Liu, S. Han, B. Lei and C. Zhou, *Nano Lett.*, 2004, **4**, 1919.
62 X. Y. Xue, Y. J. Chen, Y. G. Wang and T. H. Wang, *Appl. Phys. Lett.*, 2005, **86**, 233101.